Preparation of $MgO–MgAl_2O_4$ composite for refractory application

D. Mohapatra[a] and D. Sarkar < dsarkar@nitrkl.ac.in >

Journal of Materials Processing Technology Volume 189, Issues 1-3, 6 July 2007, Pages 279-283

http://dx.doi.org/10.1016/j.jmatprotec.2007.01.037

Preparation of $MgO–MgAl_2O_4$ composite for refractory application

D. Mohapatra, D. Sarkar *

Department of Ceramic Engineering, National Institute of Technology, Rourkela-8, Orissa, India

Abstract

Solid-state reaction was adopted to prepare MgO-rich $MgAl_2O_4$ spinel from commercially available sintered seawater magnesia and α-alumina. The starting materials were mixed in weight ratio (Al_2O_3:MgO) of 1:1, 1:1.1, 1:1.2, 1:1.3, 1:1.4. Calcination led to the development of $MgAl_2O_4$ spinel crystal seed, which was varied (5–50%) with respect to MgO content and temperature. Spinellisation of 70 vol.% was observed for equal weight proportionate calcined powder, when calcined at 1000 °C for 2 h and subsequent sintered at 1600 °C for 4 h. The initial calcination temperature and hence the primary spinel seed content was found to influence the densification and microstructure of sintered specimen. Finally attempts were made to correlate the effect of spinel seed content on the crystallization behavior and microstructure.

Keywords: Refractories; In situ spinel seed; Crystallization; Microstructure; $MgAl_2O_4$ composite; Sintering

1. Introduction

People of cement industry are affected by allergic skin ulceration and certain respiratory diseases because of the carcinogenic effect of Cr^{6+}, which presumably originates from oxidation of Cr^{3+} in magnesite–chrome and/or chrome–magnesite refractories [1,2]. In contrast, Gonsalves and Maschio et al. investigated $MgAl_2O_4$ spinel and MgO–spinel based refractories for a large number of applications as an alternative component of chrome-containing refractory [3,4]. However, the direct sintering of $MgAl_2O_4$ from their constituent oxides is very difficult because of the 5–7% volume expansion. Consequently, a two stage firing process has been employed, where first one is to complete the spinel formation and the second one is sintering at an optimum temperature to densify the formed spinel. Among this group of materials, the MgO-rich $MgAl_2O_4$ composites have significant importance for various applications and different researchers have been studying the system in depth. Bailey and Russel found that excess magnesia is beneficial for densification of spinel. The presence of periclase as a second phase restrained the grain boundary motion and produced dense, small grained body with superior mechanical characteristics [5]. Roy et al. proposed in their seminal work that a crystallographic seeding can stabilize a particular phase at higher temperature or lower the crystallization temperature, and/or to enhance the densification. The orderness, i.e. [3 1 1] phase of $MgAl_2O_4$ spinel could be increased with addition of 1.69 wt.% $MgAl_2O_4$ spinel seed and this also enhanced the percentage of spinel at low temperature when processed through chemical route [6]. Xiaolin reveals 1% crystal seeds are beneficial for the synthesis of fully crystallized $MgAl_2O_4$ spinel through sol-gel route, where initial temperature have been maintained at about 550 °C and crystallization of $MgAl_2O_4$ spinel is observed at a temperature of about 700 °C [7]. Ghosh et al. also worked on the seeding effect on synthesis of MgO-rich spinel. They reported that incorporation of 20 wt.% $MgAl_2O_4$ spinel in production of MgO refractory has great influence in improving the lower mechanical/thermo-mechanical properties [8]. Working on the development of magnesia–magnesium aluminate co-clinker, Cooper and Hudson found $MgO–MgAl_2O_4$ bricks with 40 wt.% spinel co-clinker exhibited in best combination of properties with superior resistance against thermal shock damage and possible erosion and corrosion.

By paying close attention to the earlier research work it can be emphasized that the crystallization behavior and densification of MgO-rich spinel depend on the amount of initial MgO-phase content, amount of spinel seed and/or temperature. However, the effects of in situ spinel seed content through solid-state reaction of MgO-rich $MgAl_2O_4$ spinel on crystallization and densification behavior are limited. In the present work, a wide range of MgO-rich magnesium aluminate spinel was prepared from their constituent solid-oxides at different temperatures. Phase

*

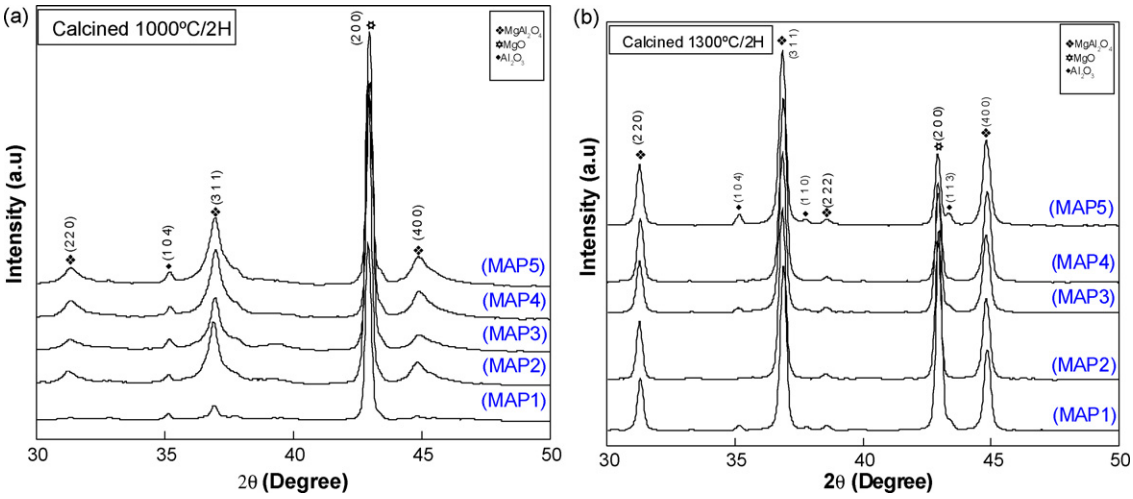

Fig. 1. XRD pattern of Al_2O_3:xMgO (where x = 1, 1.1, 1.2, 1.3 and 1.4 wt.%) powder calcined at (a) 1000 °C/2 h and (b) 1300 °C/2 h.

composition and densification parameters of the sintered products were examined at selected optimum sintering temperature. The sintered MgO-rich spinels were characterized for the crystallization behavior, extent of spinel phase development and microstructure.

2. Experimental

Seawater magnesia and commercially available α-Al_2O_3 (NALCO, India) were used as starting materials. Different batches, with weight proportion of Al_2O_3:xMgO, where x = 1, 1.1, 1.2, 1.3, 1.4 were mixed. Calcination of the different batch powders was carried out at different temperatures with 100 °C temperature interval ranging from 1000 °C to 1300 °C for 2 h soaking at peak temperature. The powders were mixed-milled with help of high dense ZrO_2 balls in acetone media. The phases in the mixed, calcined and sintered samples were analyzed using an X-ray diffractometer (Phillips PW1830, Netherlands; using Cu Kα radiation). The crystallite size 't' was determined from X-ray line broadening using the Scherer formula; $t = 0.9\lambda/B\cos\theta$, where '$t$' is the crystallite size, $B(2\theta)$ is the broadening of the diffraction line measured at half maximum intensity, λ is the wavelength of the X-ray radiation, and θ is the Bragg's angle. Line broadening due to the equipment was subtracted from the peak width before calculating the crystallite size using the following formula, $B^2 = B^2_{\text{meas}} - B^2_{\text{Equip}}$, where B_{meas} = measured full width at half maximum from peak values, B_{Inst} = Instrumental broadening.

The spinel content in the calcined as well as sintered samples was calculated from the XRD analysis using the following equation [9]:

$$\text{vol.\% of } MgAl_2O_4 = \left\{ \frac{\text{height counts of } MgAl_2O_{4\{3\,1\,1\}}}{\sum \text{height counts}(MgAl_2O_{4\{3\,1\,1\}} + MgO_{\{2\,0\,0\}} + Al_2O_{3\{1\,0\,4\}})} \right\} \times 100 \quad (1)$$

The lattice parameter was calculated [10] from

$$a = \frac{\lambda}{2\sin\theta}\sqrt{(h^2 + k^2 + l^2)} \quad (2)$$

where a is the lattice parameter, λ the radiation wavelength and $h\,k\,l$ are the corresponding Miller indices. For the study of densification behavior of the calcined powders, pellets of 12 mm in diameter were prepared by uniaxial pressing at ~275 MPa using 2 wt.% poly vinyl alcohol (PVA) as temporary binder. The pellets were heated at a rate of 5 °C/min. The study was carried out in a high temperature dilatometer (NETZSCH DL 402C) without any isothermal treatment. The green pellets (Ø 12 mm, 3 mm high) prepared using hydraulic press were taken for sintering at 1600 °C for 4 h soaking time at peak temperature. Densification study of the sintered products was performed by the conventional liquid displacement method using Archimedes' Principle in Kerosene medium. Microstructures of the polished and thermally etched samples were observed under Scanning Electron Microscope (FEI QUANTA, The Netherlands).

3. Results and discussion

Fig. 1 represents the XRD pattern of calcined powders synthesized from their constituent oxides at different temperatures. At lower temperature, all the powder exhibits broader XRD peaks of $MgAl_2O_4$ spinel phase, in addition with minor peak of unreacted corundum and sharp peaks of excess periclase phase (Fig. 1a). The crystallization of $MgAl_2O_4$ is observed at 1000 °C, which is well agreed with the earlier research work [11]. Fig. 1b reveals the trend of unreacted corundum phase, which is less in case of higher calcination temperature. Table 1 shows the calculated volume percent of $MgAl_2O_4$ formation after calcination at different temperatures. At 1000 °C, equal proportion of initial oxide

Table 1
The calculated vol.% of spinel content of calcined powders obtained from mixture of Al_2O_3:xMgO (where x = 1:1, 1:1.1, 1:1.2, 1:1.3, 1:1.4 in wt.%)

Identification	Al_2O_3:MgO	vol.% of $MgAl_2O_4$ formation after calcination at			
		1000 °C	1100 °C	1200 °C	1300 °C
MAP1	1:1.0	5.59	7.79	26.20	27.58
MAP2	1:1.1	12.23	24.17	33.20	43.97
MAP3	1:1.2	14.33	26.09	34.86	46.52
MAP4	1:1.3	18.59	38.38	46.30	48.37
MAP5	1:1.4	30.32	40.65	48.27	48.26

Table 2
Average crystallite size (nm) of spinel phase after calcination of mixed powders at different temperatures

Identification	Al_2O_3:MgO	Calcination temperature (°C)			
		1000	1100	1200	1300
MAP1	1:1.0	19.87	24.39	26.66	29.87
MAP2	1:1.1	22.80	25.15	27.96	31.91
MAP3	1:1.2	25.96	27.01	28.99	32.18
MAP4	1:1.3	26.80	28.78	30.63	32.32
MAP5	1:1.4	27.11	29.75	31.17	33.01

develops 5–6 vol.% spinel phase, whereas ~30 vol.% spinel content has been noticed for highest MgO content. The detailed phase analysis of calcined powder illustrates a gradual trend of increasing spinel formation with increasing calcination temperature as well as increasing MgO content. The phase analysis of XRD peak demonstrates ~28 and ~48 vol.% spinel phase develops at 1300 °C for the lowest and highest MgO content, respectively. Fig. 1a evidences initiation of spinel phase with broad lines, which reveals the crystallinity at this temperature is low. With increase in calcination temperature (1000–1300 °C), the diffraction peaks of spinel become sharper due to increase in the crystallinity of spinel phase (Fig. 1b). The measured crystal size for samples calcined at different temperature is listed in Table 2. The crystallite size is 19 nm for lowest calcination temperature and lowest content of MgO. However, the crystallite size gradually increases with increasing temperature and maximum 33 nm has been detected for MAP5 powder at 1300 °C for 2 h. The calculated average lattice parameter (a_0 = 8.0792 Å) of $MgAl_2O_4$ with highest MgO content has highest value. This may be due to the enlargement of spinel unit cell structure with the formation of oxygen vacant sites, i.e., spinel structure becomes anion deficient due to excess MgO [12]. The results also indicate that $MgAl_2O_4$ spinel phase develops with increasing calcination temperature.

Fig. 2 exhibits the dilatometric study of the compacted specimens up to 1250 °C without any isothermal treatment. The bar (5 mm × 5 mm × 15 mm) specimens were prepared after calcination of precursor oxides at 1000 °C for 2 h. An increase in linear expansion up to 1000 °C in all the batches indicates the starting temperature of spinel formation, which supports

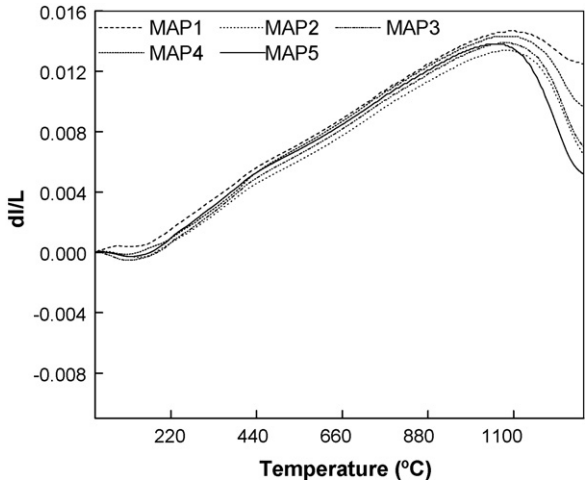

Fig. 2. Dilatometric study of green bar specimen obtained from 1000 °C/2 h calcined powders for all compositions.

the phase analysis obtained from Fig. 1a. The percentage linear change beyond 1000 °C is the combined effect of spinel formation (expansion) and densification (shrinkage). In Fig. 2, MAP5 depicts sharp fall in slope, which implies better sinterability. The presence of inherent oxygen vacancy in magnesia rich spinel composition helps the transport of oxygen ion (the rate controlling factor), resulting in greater extent of amphoteric diffusion, greater mass transport and densification [13]. The slope of MAP5 falls beyond 1000 °C is due to the exceeding densification rate over the rate of spinel formation.

Fig. 3 shows the XRD patterns of sintered samples. There is no evidence of corundum phase in all the different batches, which confirms the consumption of Al_2O_3 in formation of spinel phase, and excess MgO remains as free periclase phase. The major phases observed after sintering process in all the batches are that of $MgAl_2O_4$ (3 1 1) (2 2 0) (4 0 0) and MgO (2 0 0). The extent of spinel formation has been calculated from the XRD analysis and tabulated in Table 3. However, the total amount of spinel content of sintered specimen is low for MAS5 composition. Highest spinel phase formation in sintered specimen is noticed in presence of ~5 vol.% seed content in green pellets, and a gradual decreasing trend could be observed with increas-

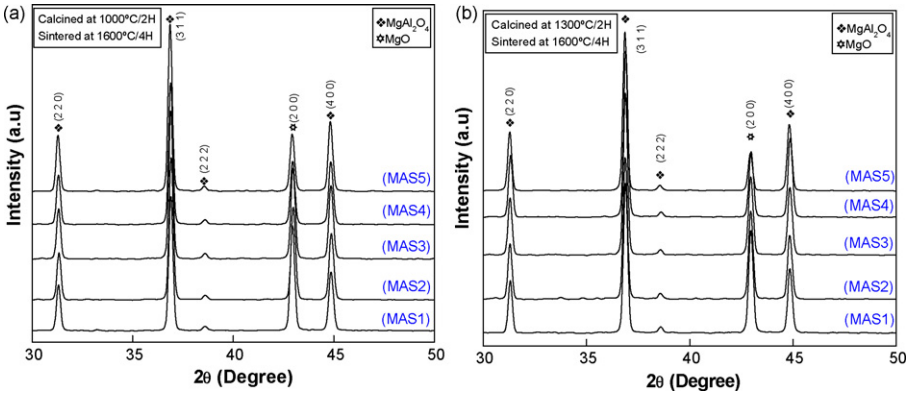

Fig. 3. XRD of sintered specimens of Al_2O_3:xMgO (where x = 1, 1.1, 1.2, 1.3 and 1.4): (a) powder calcined at 1000 °C/2 h and sintered at 1600 °C/4 h and (b) powder calcined at 1300 °C/2 h and sintered at 1600 °C/4 h.

Table 3
Spinel and MgO phase after sintering (1600 °C/4 h) of compacts obtained from calcined powders

Identification	Al_2O_3:MgO	vol.% $MgAl_2O_4$ content sintered at 1600 °C calcined at		vol.% MgO content sintered at 1600 °C calcined at	
		1000 °C	1300 °C	1000 °C	1300 °C
MAS1	1.1.0	70.54	62.36	28.12	37.64
MAS2	1:1.1	67.92	60.81	32.07	38.45
MAS3	1:1.2	65.16	58.74	34.14	40.25
MAS4	1:1.3	59.25	52.29	38.80	47.10
MAS5	1:1.4	55.49	49.56	40.74	50.03

ing initial seed content. In presence of in situ 5 vol.% spinel seed, spinellisation reaches ~70 vol.% for MAS1 at 1600 °C for 4 h through nucleation and growth process, whereas this content reduces to ~62 vol.% with increasing temperature when initial seed content is ~28 vol.%. However, with increasing MgO content, the extent of spinel phase formation decreases and reaches upto ~50 vol.%. Hence, an optimum amount of seed has significant effect on formation of MgO-rich spinel composite. This may be attributed to the effect of the content of spinel crystal seeds, which act as the substrate for heterogeneous nucleation. The rate of nucleation in a unit area of substrate is temperature dependent, and expressed as [14]:

$$I^{\mathrm{h}} = K^{\mathrm{h}} \exp\left[-\frac{\Delta G_{\mathrm{k}}^{\mathrm{h}}}{kT}\right] \tag{3}$$

where I^{h} is the rate of nucleation in a unit area of substrate, K^{h} a constant irrespective of the substrate, k the Boltzman constant, T the temperature and $\Delta G_{\mathrm{k}}^{\mathrm{h}}$ is the potential barrier for heterogeneous nucleation, which is as follows:

$$\Delta G_{\mathrm{k}}^{\mathrm{h}} = \Delta G_{\mathrm{k}} \left[\frac{1}{4}((2+\cos\theta)(1-\cos\theta)^2)\right] \tag{4}$$

where ΔG_{k} is the potential barrier for homogeneous nucleation, and θ is the contact angle between the crystal nuclei and the substrate. When the substrate is identical to the nucleating crystal, $\theta = 0$ and consequently $\Delta G_{\mathrm{k}}^{\mathrm{h}} = 0$, i.e., the potential barrier to nucleation does not exist. However, significant differences exist between the substrate and the nucleating crystal, i.e., $\theta = 180$, $\Delta G_{\mathrm{k}}^{\mathrm{h}} = \Delta G_{\mathrm{k}}$, hence, they cannot interact and therefore no acceleration of the nucleation can occur. Using this theory it can be

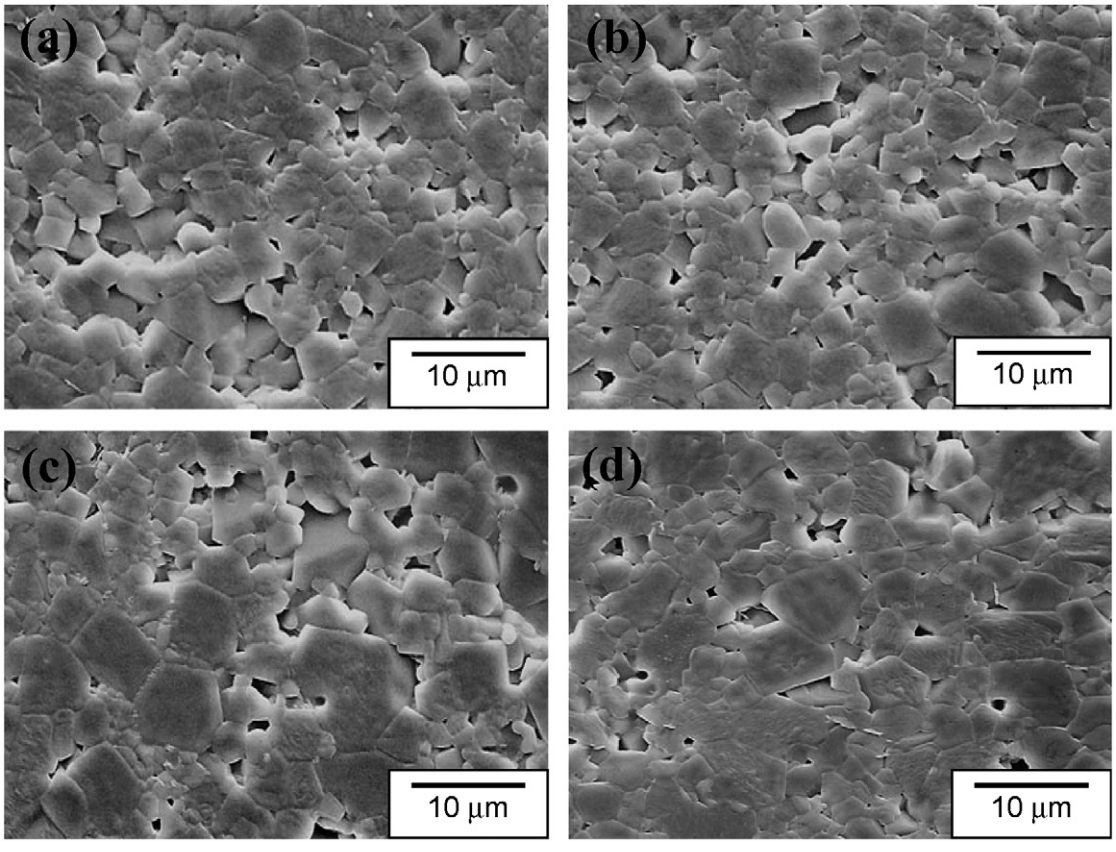

Fig. 4. SEM image of (a) MAP1 powder calcined at 1000 °C and sintered at 1600 °C/4 h, (b) MAP1 powder calcined at 1300 °C and sintered at 1600 °C/4 h, (c) MAP5 powder calcined at 1000 °C and sintered at 1600 °C/4 h and (d) MAP5 powder calcined at 1300 °C and sintered at 1600 °C/4 h.

suggested that optimum amount of $MgAl_2O_4$ crystal seeds could decrease the potential barrier for nucleation and therefore accelerate nucleation and growth of the final product ($MgAl_2O_4$) with low seed content. On the other side, the presence of excess seed accelerates the grain growth at high temperature rather than any nucleation effect. Hence, higher percentage of seed has not any advantages on the further spinel formation.

The relative density of different sample was measured after sintering of green pellets obtained from calcined powders and PVA binder. Nearly 96% relative densification was exhibited for highest MgO containing (MAS5) specimen when constituent powder was calcined at 1300 °C for 2 h and followed by sintering at 1600 °C for 4 h. The densification process is greatly influenced by calcination process, and the presence of free periclase hinders and controls the grain boundary migration. Fig. 4a and b represents the microstructure of MAS1 specimen, which are calcined at different temperature and sintered at 1600 °C/4 h. Micrograph reveals the average grain size of MAP1 calcined at 1300 °C is ∼8 μm in comparison to MAP1 calcined at 1000 °C. Similarly, Fig. 4c and d exhibits the microstructure of MAS5 with relatively larger and elongated grain at around ∼9 μm and 16 μm, when specimens were sintered after calcination at 1000 °C and 1300 °C temperature, respectively. Direct-bonded and rounded spinel–spinel grains with relatively few edges are also observed. Fig. 4a reveals that grains of MAS1 are non-uniform and pores (intergranular) are present in between the grains. The average grain size was observed to be ∼5 μm. Excess MgO suppresses the grain growth. However, some larger grain could be noticed in Fig. 4b, where content of crystal seed is ∼30 vol.%. Fig. 4d illustrates the microstructure of sample MAS5 appear to be denser with fewer pores, which confirm the results of densification parameter. The grains in sample MAS5 seem to appear as layered grains. Abnormal grain growth was identified when the powders calcined at 1300 °C and sintered at 1600 °C for 4 h. Random grain orientation and increased intergranular porosity is responsible to deteriorate the density of MAS5 specimen. From the microstructure, the average grain size ∼5 μm of MAS1 calcined at 1000 °C and sintered at 1600 °C/4 h may exhibit improved room temperature mechanical properties, whereas MAS5, calcined at 1300 °C and sintered at 1600 °C/4 h expected to provide better high temperature mechanical properties because of elongated and larger grain size.

4. Conclusions

The spinel phase development after first stage of sintering has a significant contribution on the composition and microstructure of sintered composite. Around 5 vol.% of crystal seeds of spinel is influential for the synthesis of MgO–70 vol.% $MgAl_2O_4$, whereas MgO–50 vol.% $MgAl_2O_4$ composite has been developed in presence of ∼50 vol.% initial seed content. Higher amount of crystal seeds do not influence the nucleation process rather it accelerates the grain growth at high temperature leading to reduced density. By varying the calcination temperature, the spinel phase development can be synchronized to obtain better densification and composition in sintered bodies.

References

[1] P. Bartha, in: X. Zhong, et al. (Eds.), Proceedings of the International Symposium on Refractories, Refractory Raw Materials and High Performance Refractory Products, Pergamon, Hangzhou, 1989, pp. 661–674.

[2] J.A. Reyes Sanchez, O.D. Toledo, New developments of magnesite-chrome brick and magnesite-spinel for cement rotary kilns-higher thermal shock resistance and higher coating adherence, in: Proceedings of the UNITECR 1989 Congress, Anaheim, USA, 1989, pp. 968–979.

[3] R. Dal Maschio, B. Fabbri, C. Fiori, Ind. Ceram. 8 (3) (1988) 121–126.

[4] G.E. Gonsalves, A.K. Duarte, P.O.R.C. Brant, Am. Ceram. Soc. Bull. 72 (2) (1993) 49–54.

[5] J.T. Bailey, R. Russel, Am. Ceram. Soc. Bull. 50 (5) (1971) 493–496.

[6] J.F. Pasquier, S. Komarneni, R. Roy, J. Mater. Sci. 26 (1991) 3797–3802.

[7] A. Ghosh, R. Sarkar, B. Mukherjee, S.K. Das, J. Eur. Ceram. Soc. 24 (2004) 2079–2085.

[8] S.C. Cooper, T.A. Hudson, Trans. J. Br. Ceram. Soc. 81 (4) (1982) 121–128.

[9] D. Domanski, G. Urettavizcaya, F.J. Castro, F.C. Gennari, J. Am. Ceram. Soc. 87 (11) (2004) 2020–2024.

[10] B.D. Cullity, Elements of X-ray Diffraction, 2nd ed., 1978, p. 351.

[11] M.F. Zawrah, Mater. Sci. Eng. A 382 (2004) 362–370.

[12] M. Matsui, T. Takashi, I. Oda, Effects of starting materials and calcining temperature on sintering of spinel ceramics, in: W.D. Kingery (Ed.), Advances in Ceramics, vol. 10, The American Ceramic Society, Columbus, OH, 1984, pp. 562–573.

[13] H. Kenya, O. Tadashi, N. Zenbee, Effects of starting materials and calcining temperature on sintering of spinel ceramics. Rep. Res. Lab. Eng. Mater., No. 2, Tokyo Institute of Technology, 1977, pp. 85–94.

[14] W.D. Kingery, H.K. Bowen, D.R. Uhlmann, Introduction of Ceramics, 2nd ed., John Wiley & Sons, 1991, p. 335.